

The logo for EPJ B features a dark blue rectangular background. On the left side of this background is a vertical strip with a red and orange abstract, textured pattern. The letters 'EPJ B' are printed in a large, white, serif font across the center of the blue area.

*EPJ B*

[www.epj.org](http://www.epj.org)

Condensed Matter  
and Complex Systems

Eur. Phys. J. B **63**, 493–500 (2008)

DOI: 10.1140/epjb/e2008-00265-y

## Strain-assisted spin manipulation in a quantum well

Y. Li and Y.-Q. Li



# Strain-assisted spin manipulation in a quantum well

Y. Li<sup>a</sup> and Y.-Q. Li

Zhejiang Institute of Modern Physics and Department of Physics, Zhejiang University, Hangzhou 310027, P.R. China

Received 6 March 2008 / Received in final form 28 May 2008

Published online 10 July 2008 – © EDP Sciences, Società Italiana di Fisica, Springer-Verlag 2008

**Abstract.** We show that the efficiency of manipulating electron spins in semiconductor quantum wells can be enhanced by tuning strain strengths. The combined effects of intrinsic and strain-induced spin-orbit couplings vary for different quantum wells, which provide an alternative route to understand the experimental phenomena brought in by the strain. The contribution to the electron-dipole-spin-resonance intensity induced by the strain can be changed through adjusting the direction of the  $ac$  electric field in the  $x$ - $y$  plane of the quantum well and tuning the strain strengths.

**PACS.** 71.70.Ej Spin-orbit coupling, Zeeman and Stark splitting, Jahn-Teller effect – 71.70.Fk Strain-induced splitting – 78.67.De Quantum wells – 85.75.-d Magnetoelectronics; spintronics: devices exploiting spin polarized transport or integrated magnetic fields

## 1 Introduction

Manipulating electron spins by an external electric field is a central issue in the realization of spintronics on the basis of solid-state materials [1–4] as it is important for quantum computing and information processing [5]. In a recent experiment, electron spins have been manipulated by means of a voltage-controlled  $g$ -tensor modulation technique which is applicable for materials with small  $g$  factors merely [6]. Recently, a theory of electric dipole spin resonance (EDSR) has been proposed to investigate the manipulation of electron spins in parabolic quantum wells [7,8]. An in-plane and a perpendicular electric field can be used to efficiently manipulate electron spins in quantum wells. This theory requires a tilted magnetic field but does not require the  $g$  factors to be small. On the contrary, the large  $g$  factors typical of narrow-gap  $A_3B_5$  semiconductors are advantageous for the manipulation of electron spins.

It has been recently recognized that strain-induced spin-orbit couplings can be used to effectively manipulate electron spins in the absence of applied magnetic fields, which provides an alternative route, called strain engineering, for the solid-state spin manipulation. For example, it has been employed to control the electron-spin precession [9–11] in zinc-blende structure semiconductors and to tune the spin coherence with a significant enhancement of the spin dephasing time [12]. In semiconductor epilayers, the effect of the strain on electron-spin transport [13] and that of uniaxial tensile strain on spin coherence [14,15] have also been carried out in recent experiments. The types of strain-induced spin-orbit couplings

in strained bulk semiconductors were analyzed [16] theoretically, whereas, it is not very clear so far which type of strain-induced spin-orbit couplings (i.e., Rashba-type or Dresselhaus-type) [9,16] plays an important role in manipulating electron spins. Since the spin manipulation utilizing the effect of strain can be easily realized in practical devices, it will be worthwhile to investigate the effect of strain-induced spin-orbit couplings.

In this paper, we show that the efficiency of manipulating electron spins can be enhanced through adjusting the strain strength of the semiconductor quantum wells. The combined effects of intrinsic and strain-induced spin-orbit couplings vary for different systems. We propose a method to change the contribution to the EDSR intensity through adjusting the direction of the  $ac$  electric field in the  $x$ - $y$  plane of the quantum well and tuning strain strengths. This paper is organized as follows: in the next section, we give a general consideration on the EDSR intensity caused by both intrinsic and strain-induced spin-orbit couplings. In Sections 3 and 4, we consider systems with intrinsic spin-orbit couplings of Dresselhaus type and Rashba type respectively. The spin manipulation for an InSb quantum well under strain effects is investigated in terms of the EDSR intensity. As a comparison, the combined effects of intrinsic and strain-induced spin-orbit couplings in some other kinds of semiconductor quantum wells are also studied. A summary of our main conclusion is given in the last section.

## 2 General consideration

For two-dimensional electrons in quantum wells or heterostructures of zincblende semiconductors, there exist

<sup>a</sup> e-mail: yli@hbar.zju.edu.cn

two intrinsic spin-orbit couplings called Dresselhaus and Rashba couplings that arise from the bulk-inversion asymmetry and the structure-inversion asymmetry of materials, respectively. In this paper, we investigate a heterostructure with the [001] growth direction coinciding with the  $z$  axis. The Dresselhaus spin-orbit coupling can be obtained by averaging the corresponding bulk expression over the motion relevant to the confined degree of freedom [17]. If the first electron subband is merely populated in quantum wells, the Dresselhaus type Hamiltonian  $H_{in}^D$  is given by

$$H_{in}^D = \sigma_x k_x (\lambda k_y^2 - \beta) + \sigma_y k_y (\beta - \lambda k_x^2), \quad (1)$$

where  $\beta = \lambda \langle k_z^2 \rangle$  with  $\lambda$  denoting the Dresselhaus spin-orbit coupling strength and  $\langle k_z^2 \rangle$  being averaged over the ground state. Here  $H_{in}^D$  contains both linear and cubic terms in  $k$ . In semiconductor heterostructures, there exists an additional interface contribution to the Dresselhaus spin-orbit coupling, which is absent in bulk systems [18,19]. However, the interface contribution is usually neglected in the theoretical calculations. We also neglect the interface contribution to the Dresselhaus spin-orbit coupling since the approximation does not affect our theoretical analyses.

The Rashba spin-orbit Hamiltonian can be written as [20,21],

$$H_{in}^R = \alpha (\sigma_x k_y - \sigma_y k_x), \quad (2)$$

where  $\alpha$  refers to the Rashba spin-orbit coupling strength. In some systems, the Rashba or the Dresselhaus spin-orbit coupling dominates over the other effects. In order to manipulate electron spins efficiently, it becomes important to know the relative strengths between Rashba and Dresselhaus interactions in considered systems.

In zinc-blende type semiconductors, strain can introduce an additional spin-orbit coupling which can be of structure-inversion-asymmetry type [22],

$$H_{st}^R = \frac{1}{2} C_3 [\sigma_x (\epsilon_{xy} k_y - \epsilon_{xz} k_z) + \sigma_y (\epsilon_{yz} k_z - \epsilon_{yx} k_x) + \sigma_z (\epsilon_{zx} k_x - \epsilon_{zy} k_y)]. \quad (3)$$

It can also be of bulk-inversion-asymmetry type if the diagonal components of the strain tensor  $\epsilon_{ii}$  are included

$$H_{st}^D = D [\sigma_x k_x (\epsilon_{zz} - \epsilon_{yy}) + \sigma_y k_y (\epsilon_{xx} - \epsilon_{zz}) + \sigma_z k_z (\epsilon_{yy} - \epsilon_{xx})]. \quad (4)$$

Here  $C_3$  and  $D > 0$  are material constants, and  $\epsilon_{ij}$  ( $i, j = x, y, z$ ) denote the components of the strain tensor. We call  $H_{in}^D$  and  $H_{in}^R$  in equations (1) and (2) intrinsic spin-orbit couplings so as to distinguish them from the strain-induced spin-orbit couplings in equations (3) and (4). These four types of spin-orbit couplings may take place simultaneously if strain is exerted on a sample. However, they can play different roles in manipulating electron spins. It is worthwhile to study which kind of strain-induced spin-orbit couplings plays an important role in spin manipulation in various semiconductor quantum wells.

In order to carry out a general calculation of the EDSR intensity for semiconductor quantum wells with spin-orbit couplings, we consider

$$H = H_0 + H_{so} + e\mathbf{E}(t) \cdot \mathbf{r}, \quad (5)$$

which describes two-dimensional electrons with the spin-orbit coupling in a parabolic quantum well. An in-plane  $ac$  electric field  $\mathbf{E}(t) = E(t)(\cos \phi, \sin \phi, 0)$  and a tilted magnetic field  $\mathbf{B}(\theta, \varphi)$  with  $\theta$  and  $\varphi$  being the polar and azimuthal angle of  $B$  together with a strain are applied to the system. Accordingly, the first term in equation (5) reads

$$H_0 = \frac{1}{2m^*} \left( \mathbf{p} + \frac{e}{c} \mathbf{A} \right)^2 + \frac{1}{2} m^* \omega_0^2 z^2 + \frac{g}{2} \mu_B \sigma \cdot \mathbf{B},$$

where  $\mathbf{A}$  is the vector potential of the tilted magnetic field,  $m^*$  denotes the effective electron mass, and  $\omega_0$  characterizes the parabolic potential well. The second term  $H_{so}$  in equation (5) may include both intrinsic and strain-induced spin-orbit couplings.

It was noticed that [23,24] the anisotropy of the  $g$  factor depends on the spin-orbit coupling and the external magnetic field. While, we do not take the anisotropy of the  $g$  factor into account in this paper since for the systems considered here the spin-orbit coupling energy is relatively small in comparison to other energy scales, such as the confinement energy  $\hbar\omega_0$ , the cyclotron energy  $\hbar\omega_c = \hbar eB/m^*c$  and the Zeeman-splitting energy  $\hbar\omega_z = g\mu_B B$ . In order to derive an explicit expression for the spin-flip transition probabilities, we assume parabolic bands by omitting the contribution of the higher order terms to the effective mass [18,25,26]. The nonparabolic effects of the bands can be evaluated by a further approximation treatment.

To diagonalize the Hamiltonian  $H_0$ , one needs to rotate the original coordinate frame  $\{\hat{x}, \hat{y}, \hat{z}\}$  to the new one  $\{\hat{x}', \hat{y}', \hat{z}'\}$ , where  $\hat{z}'$  is chosen in alignment with the orientation of  $\mathbf{B}$ ,  $\hat{y}'$  is lying in  $x$ - $y$  plane, and  $\hat{x}'$  is chosen to form a right-hand triple with  $\hat{y}'$  and  $\hat{z}'$ . Thus the coordinates in both frame systems are related,  $(\hat{x}, \hat{y}, \hat{z}) = (\hat{x}', \hat{y}', \hat{z}')R^T$ , by

$$R = \begin{pmatrix} \cos \theta \cos \varphi, & -\sin \varphi, & \sin \theta \cos \varphi \\ \cos \theta \sin \varphi, & \cos \varphi, & \sin \theta \sin \varphi \\ -\sin \theta, & 0, & \cos \theta \end{pmatrix},$$

which also relates the momentum components in the two frame systems,  $k_i = R_{ij} k'_j$  (here  $i, j = x, y, z$ ). By using the Landau gauge  $\mathbf{A} = (0, Bx', 0)$ ,  $H_0$  can be written as the sum of two harmonic oscillators [8] and its energy levels are given by

$$E_s(n_+, n_-) = \hbar\omega_+ \left( n_+ + \frac{1}{2} \right) + \hbar\omega_- \left( n_- + \frac{1}{2} \right) + \frac{s}{2} \hbar\omega_z, \quad (6)$$

where  $s = \pm 1$  label the spin states and  $n_{\pm}$  refer to the orbital quantum numbers,  $\omega_{\pm}(\theta)$  are the frequencies of

$$\begin{aligned}
T^{\text{D+R}} = & -\frac{\lambda}{\hbar Q_3} \sum_{\nu=+,-} \left\{ [\omega_c \cos(\varphi - \phi) \cos \theta + i \omega_z \sin(\varphi - \phi)] \Omega Q_\nu Q_1 \right. \\
& + [\Omega \omega_c \cos \theta \sin(\varphi - \phi) - i \omega_z \cos(\varphi - \phi) (\Omega + \omega_c^2 \sin^2 \theta)] Q_\nu Q_2 \left. \right\} + \frac{\beta}{\hbar Q_3} \left\{ \cos(\varphi - \phi) \right. \\
& [\Omega \omega_c \cos \theta (i \cos 2\varphi - \sin 2\varphi \cos \theta) + \omega_z (\Omega + \omega_c^2 \sin^2 \theta) (\sin 2\varphi - i \cos 2\varphi \cos \theta)] \\
& \left. + i \sin(\varphi - \phi) \Omega [\omega_z (i \cos 2\varphi - \sin 2\varphi \cos \theta) + \omega_c \cos \theta (\sin 2\varphi - i \cos 2\varphi \cos \theta)] \right\} \\
& - \frac{\gamma}{\hbar Q_3} \left\{ \cos(\varphi - \phi) [\Omega \omega_c \cos^2 \theta + \omega_z (\Omega + \omega_c^2 \sin^2 \theta)] + i \cos \theta \sin(\varphi - \phi) (\omega_c + \omega_z) \Omega \right\}, \quad (11)
\end{aligned}$$

the coupled cyclotron-confinement modes

$$\begin{aligned}
\omega_{\pm}^2(\theta) &= \frac{\omega_0^2 + \omega_c^2 \pm \Delta^2 \operatorname{sgn}(\omega_0 - \omega_c)}{2}, \\
\Delta^2 &= (\omega_0^4 + \omega_c^4 - 2\omega_0^2 \omega_c^2 \cos 2\theta)^{1/2}. \quad (7)
\end{aligned}$$

Since the spin-orbit coupling energy is relatively small in comparison to other energy scales, one can calculate the EDSR intensity by employing the method proposed in reference [8]. The strategy of this method is to eliminate the terms related to spin-orbit couplings in the original Hamiltonian with the help of a canonical transformation  $e^F$ . After some algebraic calculations, the operators of coordinates and momenta in the original coordinates can be expressed as linear combinations of the creation and annihilation operators of the harmonic oscillators. Furthermore, the spin-orbit coupling  $H_{so}$  and the interaction term  $e\mathbf{E}(t) \cdot \mathbf{r}$  can be expressed in terms of the creation and annihilation operators. The EDSR intensity  $I \propto |T|^2$  is obtained by evaluating the matrix elements  $T$  which characterize the spin-flip transitions induced by the  $ac$  electric field  $\mathbf{E}(t)$ , namely,

$$T = \frac{1}{E(t)} \langle n_+, n_-, \uparrow | \mathbf{E}(t) \cdot [\hat{F}, \mathbf{r}] | n_+, n_-, \downarrow \rangle. \quad (8)$$

Here the operator  $\hat{F}$  is perturbatively determined by the following relation

$$\begin{aligned}
\langle n'_+, n'_-, s' | \hat{F} | n_+, n_-, s \rangle = \\
\frac{\langle n'_+, n'_-, s' | H_{so} | n_+, n_-, s \rangle}{E_{s'}(n'_+, n'_-) - E_s(n_+, n_-)} + \text{high order}. \quad (9)
\end{aligned}$$

This is the condition for the cancellation of the spin-orbit coupling term  $H_{so}$  with the first order (or further orders if necessary) perturbation terms brought in by the canonical transformation  $e^{\hat{F}}$ , which connects the eigenstates of  $H_0 + H_{so}$  with the eigenstates of  $H_0$ . Note that the Pauli matrices as well as  $\mathbf{r}$  in equation (5) are with respect to the original coordinate frame  $\{\hat{x}, \hat{y}, \hat{z}\}$ . They should also be reexpressed with respect to the new coordinate frame  $\{\hat{x}', \hat{y}', \hat{z}'\}$  so that equations (8) and (9) are computable.

## 3 Systems with intrinsic Dresselhaus coupling

### 3.1 Strain-induced Rashba-type coupling

We firstly consider the strain-induced Rashba-type spin-orbit coupling for the systems with intrinsic Dresselhaus coupling (we call D + R case for brevity). A concrete example of such a system is an InSb quantum well [27], where  $H_{in}^{\text{D}}$  dominates over  $H_{in}^{\text{R}}$  with typical value  $\lambda = 200 \text{ eV \AA}^3$  [28]. The spin precession for two dimensional electrons in the InSb quantum well is described by the following Hamiltonian

$$\begin{aligned}
H_{so}^{\text{D+R}} &= H_{in}^{\text{D}} + H_{st}^{\text{R}} \\
&= \beta(\sigma_y k_y - \sigma_x k_x) + \gamma(\sigma_x k_y - \sigma_y k_x) \\
&\quad + \lambda(\sigma_x k_x k_y^2 - \sigma_y k_y k_x^2), \quad (10)
\end{aligned}$$

where the strain parameter  $\gamma = \frac{1}{2} C_3 \epsilon_{xy}$ , the uniaxial strain is along the [110] direction ( $\epsilon_{xy} = \epsilon'_{110}/2$ , with all other off-diagonal elements vanishing),  $C_3 = 1.13 \times 10^{-7} \text{ eV cm}$  [29,30] and the electric field is in-plane ( $\langle k_z \rangle = 0$ ). Another contribution including the diagonal elements of the strain tensor  $\epsilon_{ii}$  exists, but is negligibly small according to reference [31]. The former two terms in equation (10) are linear in momenta so that they appear as linear combinations of the creation and annihilation operators in the new coordinate frame. The last term is cubic in  $k$  for which we only need to keep those parts with nonvanishing contribution to the matrix elements of equation (8). As we have kept the term proportional to  $\lambda$  in the original Hamiltonian, we have to account for the second order terms appearing after the canonical transformation. After tedious calculations, we find that the term proportional to  $\gamma\beta$  vanishes while the term proportional to  $\lambda$  remains. As a result, in the lowest energy level,  $n_+ = n_- = 0$ , we obtain from the formula (8) that

see equation (11) above

where

$$\begin{aligned}
Q_1 &= \left( \frac{\cos \theta}{2} + i \cot 2\varphi \right) Q_4 + (\cos \theta \sin 2\varphi - i \cos 2\varphi) \\
&\quad \times \left( 1 - \frac{\omega_+^2}{\omega_c^2} \right) \frac{\omega_c^2}{\Delta^2} \operatorname{sgn}(\omega_0 - \omega_c), \\
Q_2 &= \frac{3}{2} i Q_4 + (\cos \theta \cos 2\varphi + i \sin 2\varphi) \\
&\quad \times \left( 1 - \frac{\omega_{\pm}^2}{\omega_c^2} \right) \frac{\omega_c^2}{\Delta^2} \operatorname{sgn}(\omega_0 - \omega_c),
\end{aligned}$$

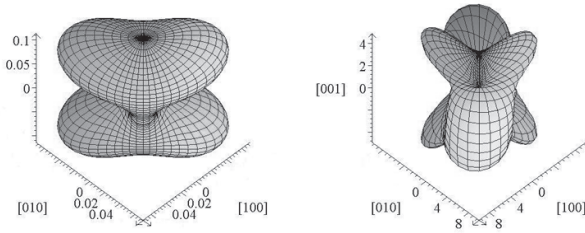


**Fig. 1.** The angular dependence of the EDSR intensity  $I(\theta, \varphi)$  (arb.units) is plotted for a [001] InSb quantum well with the strain component  $\epsilon_{xy} = 0$  (left panel) and  $\epsilon_{xy} = 0.13\%$  (right panel). Other parameters are taken as  $\omega_c/\omega_0 = 0.5$ ,  $\omega_z/\omega_0 = -0.16$ ,  $\beta = 1$ ,  $\phi = \pi/4$ , an imaginary part  $i\delta$  ( $\delta = 0.05\omega_0$ ) is added to  $Q_3$  to eliminate the divergent pole.

$$\begin{aligned}
 Q_3 &= \omega_0^2(\omega_c^2 \cos^2 \theta - \omega_z^2) - \omega_z^2(\omega_c^2 - \omega_z^2), \\
 Q_4 &= -\frac{\omega_c^2}{\Delta^2} \sin 2\varphi \sin^2 \theta \operatorname{sgn}(\omega_0 - \omega_c), \\
 Q_{\pm} &= m^* \omega_{\pm} / 2\hbar, \\
 \Omega &= \omega_0^2 - \omega_z^2.
 \end{aligned}$$

The terms proportional to  $\beta$  and  $\gamma$  in equation (11) are in agreement with the results [8] for pure Dresselhaus and Rashba spin-orbit couplings. Note that strain-induced Dresselhaus and Rashba spin-orbit couplings can result in similar contribution terms. Then it is not difficult to understand the matrix elements of the spin-flip transition in the following parts.

Firstly, we investigate the angular dependence of the EDSR intensity for the InSb-based strained quantum well. In Figure 1, we present the EDSR intensity as a function of the magnetic field direction  $\theta$  and  $\varphi$  with the fixed direction of the electric field  $\mathbf{E} \parallel [110]$  ( $\phi = \pi/4$ ). In our calculations, the system's parameters are chosen by referring to experimental situations, i.e.,  $\lambda = 200 \text{ eV}\text{\AA}^3$ ,  $C_3 = 1.13 \times 10^{-7} \text{ eV cm}$ ,  $\omega_z/\omega_c = -0.32$ ,  $\omega_0 = 2eB_0/(m^*c)$  with  $B_0 = 2 \text{ T}$ ,  $\beta = \lambda \langle k_z^2 \rangle = \lambda m^* \omega_0 / (2\hbar)$  and  $m^* = 0.014m_0$  with  $m_0$  being the mass of the free electron. We set  $\beta = 1$  and an imaginary part  $i\delta$  ( $\delta = 0.05\omega_0$ ) is added to  $Q_3$  to eliminate the divergent pole in the numerical calculation. As illustrated in the left panel of Figure 1, the EDSR intensity increases when the magnetic field is tilted with small polar angle  $\theta$  and the strain component  $\epsilon_{xy}$  is zero. This feature implies that the manipulation of electron spins becomes more efficient with a tilted magnetic field. It is seen from the left panel of Figure 1 that the EDSR intensity possesses a twofold symmetry. Since the linear term of  $H_{in}^D$  possesses a symmetric group  $C_{2v}$ , the second term in equation (11), which is the dominant contribution to the EDSR intensity in the absence of strain, has a twofold symmetry. Therefore, the EDSR intensity, which is proportional to the module square of the matrix element T, exhibits a fourfold symmetry. However, when the direction of  $\mathbf{E}$  is fixed at  $\phi = \pi/4$ , the EDSR intensity has only a twofold symmetry as illustrated in the left panel of Figure 1, in agreement with the result of reference [8]. The effect of the strain-induced spin-orbit cou-

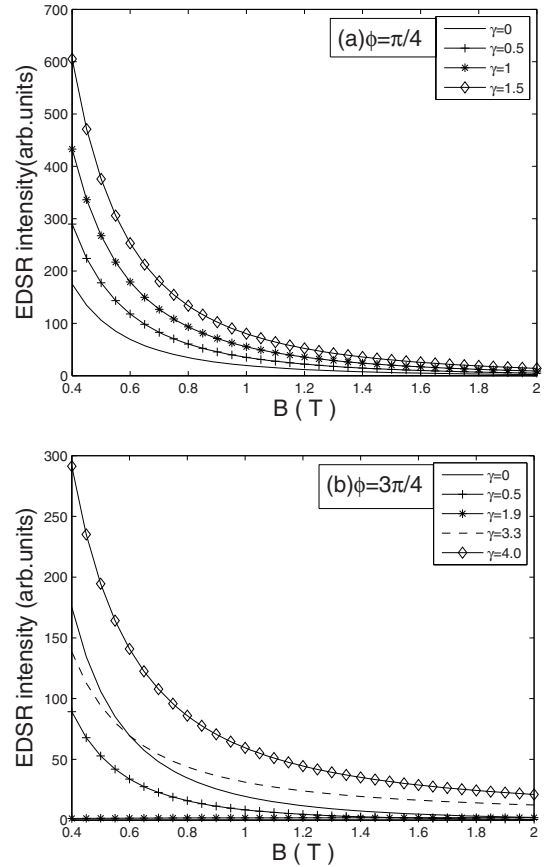


**Fig. 2.** The EDSR intensities versus the magnetic field in the D + R case are plotted for two different directions of the  $ac$  electric field (a)  $\phi = \pi/4$  and (b)  $\phi = 3\pi/4$  with different strain strengths. Other parameters are taken as  $m^* = 0.014m_0$ ,  $\omega_z/\omega_c = -0.32$ ,  $\theta = 0$ ,  $\varphi = 0$ ,  $\beta = 1$ ,  $\epsilon_{xy} = \gamma \times \epsilon_0$ , and  $\epsilon_0 = 2\beta/C_3 = 0.13\%$ .

pling is presented in the right panel of Figure 1. The strain component is  $\epsilon_{xy} = 2\beta/C_3 = 0.13\%$  and the direction of  $\mathbf{E}$  is also fixed at  $\phi = \pi/4$ . It is obvious that the maximum of the EDSR intensity can be increased significantly under strain effects. The increment of the EDSR intensity means that the strain-induced spin-orbit coupling can be used to enhance the efficiency of spin manipulation of electrons. We can find that the EDSR intensity possesses only a twofold symmetry. The twofold symmetry of the EDSR intensity arises from the combined action of the Rashba spin-orbit coupling and the linearized Dresselhaus spin-orbit coupling.

Figure 2 illustrates the magnetic field dependence of the EDSR intensity. The magnetic field perpendicular to  $x$ - $y$  plane of the quantum well, namely  $\theta = 0$  and  $\varphi = 0$ , is introduced for a conveniently experimental measurement. The direction of the  $ac$  electric field is fixed at  $\phi = \pi/4$  or  $\phi = 3\pi/4$ . Here, the unit of the EDSR intensity is  $1/\hbar^2\omega_0^2$  with  $\omega_0$  being the same value as the one in Figure 1; the other parameters are chosen as  $m^* = 0.014m_0$ ,  $\omega_z/\omega_c = -0.32$ ,  $\beta = 1$ ,  $\epsilon_{xy} = \gamma \times \epsilon_0$  and  $\epsilon_0 = 2\beta/C_3 = 0.13\%$ . As shown in Figure 2a, the maximum of the EDSR intensity

monotonously increases from 170 units to about 600 units as the strain strength increases from  $\epsilon_{xy} = 0$  to  $\epsilon_{xy} = 0.195\%$  for  $\phi = \pi/4$ . However, when the direction of the  $ac$  electric field  $\phi$  is tuned from  $\phi = \pi/4$  to  $\phi = 3\pi/4$ , the strain dependence of the EDSR intensity is changed as illustrated in Figure 2b. The solid line shows that the maximum of the EDSR intensity is about 170 units in the strain-free case (i.e.,  $\gamma = 0$ ). With the increment of the strain strength, the EDSR intensity firstly decreases to zero when the strain strength is  $\epsilon_{xy} = 0.247\%$  (i.e.,  $\gamma \approx 1.9$ ), then turns to increase after the strain strength exceeds  $\epsilon_{xy} = 0.247\%$  and reaches 300 units when  $\gamma = 4.0$ . Values of the strain strength between  $0.04\%$ – $0.46\%$  has already been experimentally realized [9,16].

Let us make a qualitative analysis with respect to the above strain dependence of the EDSR intensity. The contribution of the first term in equation (11) is relatively small in comparison to the other terms when the well width is small and/or the temperature is sufficiently low, thus it can be neglected for a qualitative estimation. Then the matrix element of the spin-flip transition in equation (11) dominates

$$T^{\text{D+R}} \propto \frac{1}{\omega_c^2 - \omega_z^2} [\beta(i \cos \phi - \sin \phi)(\omega_c - \omega_z) - \gamma(\cos \phi - i \sin \phi)(\omega_c + \omega_z)].$$

Consequently, the EDSR intensity behaves as

$$I^{\text{D+R}}(\phi) \propto \frac{1}{(\omega_c^2 - \omega_z^2)^2} [\gamma^2(\omega_c + \omega_z)^2 + \beta^2(\omega_c - \omega_z)^2 + 2\gamma\beta \sin 2\phi(\omega_c^2 - \omega_z^2)]. \quad (12)$$

It is obvious that the EDSR intensity approaches to zero when  $\gamma = (\omega_c - \omega_z)\beta/(\omega_c + \omega_z) = 1.94\beta$  for  $\phi = 3\pi/4$ . From this equation, one can see that the EDSR intensity increases monotonously for  $\phi = \pi/4$  while it firstly decreases and then increases for  $\phi = 3\pi/4$  as the strain strength increases. The dependence of the EDSR intensity on the direction of the  $ac$  electric field is plotted in Figure 3, which shows a sinusoid-like behavior with amplitude and central value being determined by the strain strength.

We also calculate the EDSR intensity when the magnetic field is tilted ( $\theta \neq 0$ ). The strain dependences of the EDSR intensity are similar to the cases at  $\theta = 0$ . Therefore electron spins can be sufficiently manipulated by using an  $ac$  electric field for the inversion asymmetry semiconductor quantum wells exerted with an appropriate strain.

The theoretical results above obtained could be experimentally measured. For this purpose, one may consider such a geometry that the InSb quantum well suffers from compression along the [110] direction. The  $ac$  electric field  $\mathbf{E}(t)$  is in the plane of the 2DEG, and the magnetic field is perpendicular to the plane. A permanent uniaxial stress can be applied to the sample either with the help of a screw putting in the sample holder or by means of other mechanical methods [15]. In the former approach, the strength of the uniaxial stress to the sample can be

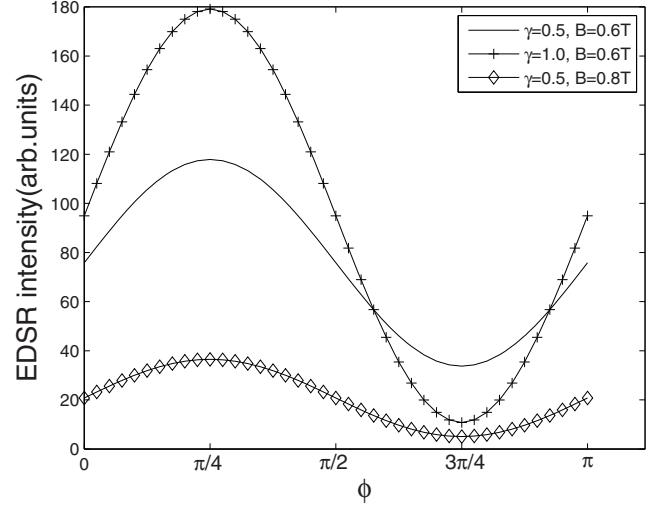


**Fig. 3.** The EDSR intensities versus the direction of the  $ac$  electric field  $\phi$  are plotted in the D + R case. Other parameters are taken as  $m^* = 0.014m_0$ ,  $\omega_z/\omega_c = -0.32$ ,  $\theta = 0$ ,  $\varphi = 0$ ,  $\beta = 1$ ,  $\epsilon_{xy} = \gamma \times \epsilon_0$  and  $\epsilon_0 = 2\beta/C_3 = 0.13\%$ .

varied by adjusting the screw before structural failure occurs. One can measure the EDSR intensities for the  $ac$  electric field along the  $\phi = \pi/4$  ([110]) and  $3\pi/4$  ([ $\bar{1}\bar{1}0$ ]) directions under certain strain strength. The measurement of the EDSR intensity by tuning the strength of the uniaxial stress could be used to accomplish the verification of the theoretical results. The other approach is due to the fact that the strain on samples can be realized in terms of a technique in growing by molecular beam epitaxy. A group of samples with different strain strengths [9,16] can be used to measure the EDSR intensity and to verify the theoretical results.

### 3.2 Strain-induced Dresselhaus-type coupling

As a comparison, we consider other kinds of semiconductor quantum wells. If the spin-orbit coupling induced by strain is assumed to be Dresselhaus-type, namely  $H_{st}^{\text{D}}$ , while  $H_{in}^{\text{D}}$  is still dominant over  $H_{in}^{\text{R}}$  in these quantum wells, the total Hamiltonian describing the spin precession of electrons in such quantum wells (call D + D case for brevity) is written as

$$\begin{aligned} H_{so}^{\text{D+D}} &= H_{in}^{\text{D}} + H_{st}^{\text{D}} \\ &= \sigma_x k_x (\lambda k_y^2 - \beta) + \sigma_y k_y (\beta - \lambda k_x^2) \\ &\quad + \gamma_1 (\sigma_x k_x - \sigma_y k_y), \end{aligned} \quad (13)$$

with the strain configuration  $\epsilon_{xx} = \epsilon_{yy}$  and  $\gamma_1 = D(\epsilon_{zz} - \epsilon_{xx}) > 0$ . The parameters  $\lambda$ ,  $\beta$  and  $\gamma_1$  are different for different kinds of quantum wells. In the following part of this paper, we do not consider concrete materials in the numerical calculation. In the lowest energy level,  $n_+ = n_- = 0$ , the matrix element of the spin-flip transition

$$\begin{aligned}
T^{D+D} = & -\frac{\lambda}{\hbar Q_3} \sum_{\nu=+,-} \left\{ [\omega_c \cos(\varphi - \phi) \cos \theta + i\omega_z \sin(\varphi - \phi)] \Omega Q_\nu Q_1 \right. \\
& + [\Omega \omega_c \cos \theta \sin(\varphi - \phi) - i\omega_z \cos(\varphi - \phi) (\Omega + \omega_c^2 \sin^2 \theta)] Q_\nu Q_2 \left. \right\} \\
& + \frac{(\beta - \gamma_1)}{\hbar Q_3} \left\{ \cos(\varphi - \phi) [\Omega \omega_c \cos \theta (i \cos 2\varphi - \sin 2\varphi \cos \theta) + \omega_z (\Omega + \omega_c^2 \sin^2 \theta) (\sin 2\varphi - i \cos 2\varphi \cos \theta)] \right. \\
& \left. + i \sin(\varphi - \phi) \Omega [\omega_z (i \cos 2\varphi - \sin 2\varphi \cos \theta) + \omega_c \cos \theta (\sin 2\varphi - i \cos 2\varphi \cos \theta)] \right\}. \quad (14)
\end{aligned}$$

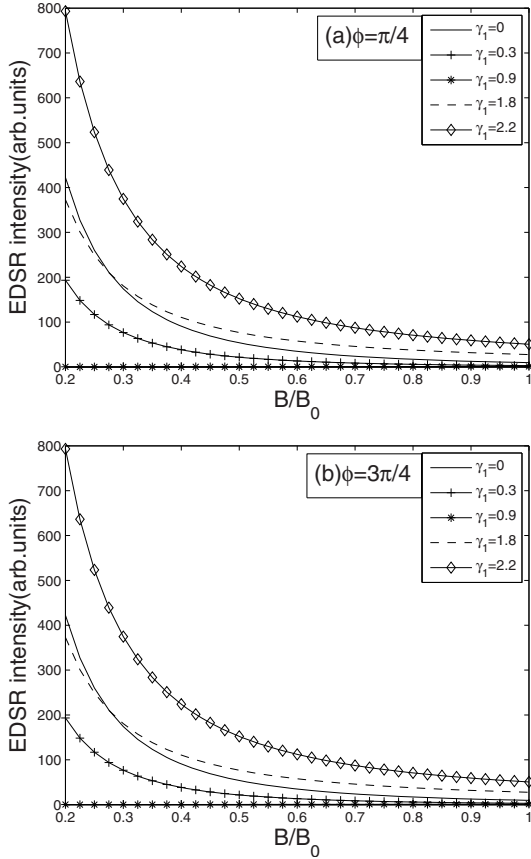


**Fig. 4.** The EDSR intensities versus the magnetic field in the D + D case are plotted for (a)  $\phi = \pi/4$  and (b)  $\phi = 3\pi/4$ . Here  $B_0 = \omega_0 m^* c/2e$  and other parameters are taken as  $\omega_z/\omega_c = -0.32$ ,  $\theta = 0$ ,  $\varphi = 0$ ,  $\beta = 1$ ,  $\epsilon_{zz} - \epsilon_{xx} = \gamma_1 \times \gamma_{10}/D$  and  $\gamma_{10} = \beta$ .

$T^{D+D}$  for  $H_{so}^{D+D}$  is calculated by using the similar method employed in previous subsection,

see equation (14) above

The EDSR intensity as a function of the magnetic field is presented in Figure 4 in the D + D case. The system's parameters are chosen as  $\omega_z/\omega_c = -0.32$ ,  $B_0 = \omega_0 m^* c/2e$ ,  $\theta = 0$ ,  $\varphi = 0$ ,  $\beta = 1$ ,  $\epsilon_{zz} - \epsilon_{xx} = \gamma_1 \times \gamma_{10}/D$  and  $\gamma_{10} = \beta$ . Although the ratio  $\omega_z/\omega_c$  may differ for different quantum wells, the feature of the curves in Figure 4 can present the strain dependence of the EDSR intensity in the D + D case. With the increment of the strain strength, as shown in Figure 4, the EDSR intensity decreases firstly. After the strain strength exceeds certain value ( $\gamma_1 \simeq 0.9$ ), it turns

to increase for both directions  $\phi = \pi/4$  and  $\phi = 3\pi/4$ . The strain dependence of the EDSR intensity can also be analyzed qualitatively. The matrix element of the spin-flip transition in equation (14) dominates

$$T^{D+D} \propto \frac{(\beta - \gamma)(i \cos \phi - \sin \phi)}{\omega_c + \omega_z}.$$

Consequently, the EDSR intensity behaves as  $I^{D+D}(\phi) \propto (\beta - \gamma)^2/(\omega_c + \omega_z)^2$ , which is independent of the direction of the  $ac$  electric field. Obviously the EDSR intensity approaches to zero when  $\gamma \simeq \beta$ . Note that the relatively small contribution of the first term in equation (14) has to be considered.

#### 4 Systems with intrinsic Rashba coupling

In this section, we investigate the strain dependence of the EDSR intensity for quantum wells with the intrinsic Rashba-type spin-orbit coupling, which is described by the Hamiltonian  $H_{in}^R$ . Since the strain can introduce the Rashba-type and Dresselhaus-type spin-orbit couplings, namely  $H_{st}^R$  and  $H_{st}^D$ , the total Hamiltonians corresponding to the R + R and R + D cases are, respectively,

$$\begin{aligned}
H_{so}^{R+R} &= (\alpha + \gamma)(\sigma_x k_y - \sigma_y k_x), \\
H_{so}^{R+D} &= \alpha(\sigma_x k_y - \sigma_y k_x) + \gamma_1(\sigma_x k_x - \sigma_y k_y). \quad (15)
\end{aligned}$$

Here the definitions of parameters  $\alpha$ ,  $\gamma$  and  $\gamma_1$  are the same as those forementioned, while their magnitudes depend on concrete materials and the strain configurations. The Hamiltonians in equations (15) describe the systems with strain-induced Rashba-type and Dresselhaus-type spin-orbit couplings, respectively. Their corresponding matrix elements of the spin-flip transition  $T^{R+R}$  and  $T^{R+D}$  are respectively obtained,

$$\begin{aligned}
T^{R+R} = & -\frac{(\gamma + \alpha)}{\hbar Q_3} \left\{ \cos(\varphi - \phi) \right. \\
& \left. [\Omega \omega_c \cos^2 \theta + \omega_z (\Omega + \omega_c^2 \sin^2 \theta)] \right. \\
& \left. + i \cos \theta \sin(\varphi - \phi) (\omega_c + \omega_z) \Omega \right\}, \quad (16)
\end{aligned}$$

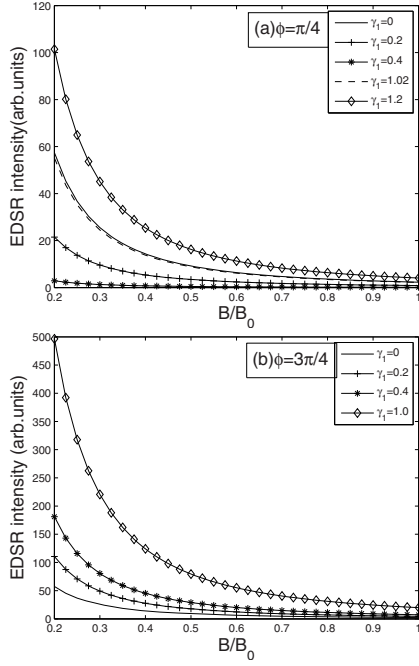


**Fig. 5.** The EDSR intensities versus the magnetic field in the R + D case are plotted for (a)  $\phi = \pi/4$  and (b)  $\phi = 3\pi/4$ . Here  $B_0 = \omega_0 m^* c / 2e$  and other parameters are taken as  $\omega_z / \omega_c = -0.32$ ,  $\theta = 0$ ,  $\varphi = 0$ ,  $\alpha = 1$ ,  $\epsilon_{zz} - \epsilon_{xx} = \gamma_1 \times \gamma'_{10} / D$  and  $\gamma'_{10} = \alpha$ .

$$\begin{aligned}
 T^{\text{R+D}} = & \frac{-\gamma_1}{\hbar Q_3} \left\{ \cos(\varphi - \phi) \right. \\
 & \times [\Omega \omega_c \cos \theta (i \cos 2\varphi - \sin 2\varphi \cos \theta) \\
 & + \omega_z (\Omega + \omega_c^2 \sin^2 \theta) (\sin 2\varphi - i \cos 2\varphi \cos \theta)] \\
 & + i \sin(\varphi - \phi) \Omega [\omega_z (i \cos 2\varphi - \sin 2\varphi \cos \theta) \\
 & + \omega_c \cos \theta (\sin 2\varphi - i \cos 2\varphi \cos \theta)] \left. \right\} \\
 & - \frac{\alpha}{\hbar Q_3} \left\{ \cos(\varphi - \phi) [\Omega \omega_c \cos^2 \theta \right. \\
 & + \omega_z (\Omega + \omega_c^2 \sin^2 \theta)] \\
 & \left. + i \cos \theta \sin(\varphi - \phi) (\omega_c + \omega_z) \Omega \right\}. \quad (17)
 \end{aligned}$$

For the R + R case, one can see from equation (16) that both the EDSR intensities increase monotonously as the strain strengths increase for the two directions  $\phi = \pi/4$  and  $\phi = 3\pi/4$ , because  $T^{\text{R+R}} \propto (\gamma + \alpha)(i \sin \phi - \cos \phi) / (\omega_c - \omega_z)$ . The EDSR intensity is  $I^{\text{R+R}}(\phi) \propto (\alpha + \gamma)^2 / (\omega_c - \omega_z)^2$ , which is also independent of the direction of the  $ac$  electric field.

For the R + D case, using  $T^{\text{R+D}}$  in equation (17), the magnetic field dependence of the EDSR intensity is represented in Figure 5. The parameters are chosen as  $\omega_z / \omega_c = -0.32$ ,  $B_0 = \omega_0 m^* c / 2e$ ,  $\theta = 0$ ,  $\varphi = 0$ ,  $\alpha = 1$ ,  $\epsilon_{zz} - \epsilon_{xx} = \gamma_1 \times \gamma'_{10} / D$  and  $\gamma'_{10} = \alpha$ . Clearly, the maximum of the EDSR intensity firstly decreases from 55 units in the strain-free case (i.e.,  $\gamma_1 = 0$ ) to zero ( $\gamma_1 \simeq 0.4$ ) for  $\phi = \pi/4$  (see Fig. 5a). As shown in Figure 5b, the EDSR intensity increases monotonously with the increment of

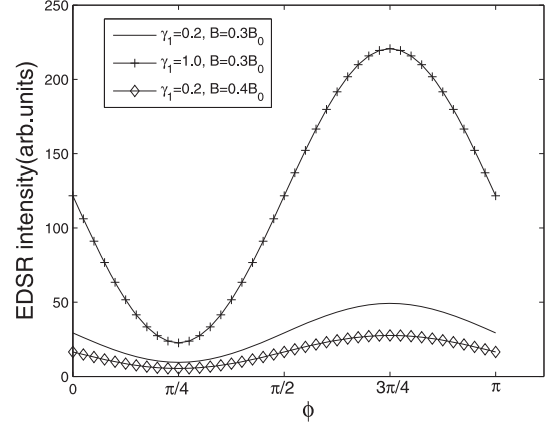


**Fig. 6.** The EDSR intensities versus the direction of the  $ac$  electric field  $\phi$  are plotted in the R + D case. Here  $\omega_0 = 2eB_0 / (m^* c)$  and other parameters are taken as  $\omega_z / \omega_c = -0.32$ ,  $\theta = 0$ ,  $\varphi = 0$ ,  $\alpha = 1$ ,  $\epsilon_{zz} - \epsilon_{xx} = \gamma_1 \times \gamma'_{10} / D$  and  $\gamma'_{10} = \alpha$ .

the strain strength for  $\phi = 3\pi/4$ . The strain dependence of the EDSR intensity can also be analyzed qualitatively. The matrix element of the spin-flip transition in equation (17) dominates

$$\begin{aligned}
 T^{\text{R+D}} \propto & \frac{1}{\omega_c^2 - \omega_z^2} [-\gamma_1 (i \cos \phi - \sin \phi) (\omega_c - \omega_z) \\
 & - \alpha (\cos \phi - i \sin \phi) (\omega_c + \omega_z)].
 \end{aligned}$$

Consequently, the EDSR intensity behaves as

$$\begin{aligned}
 I^{\text{R+D}}(\phi) \propto & \frac{1}{(\omega_c^2 - \omega_z^2)^2} [\alpha^2 (\omega_c + \omega_z)^2 + \gamma_1^2 (\omega_c - \omega_z)^2 \\
 & - 2\alpha \gamma_1 \sin 2\phi (\omega_c^2 - \omega_z^2)]. \quad (18)
 \end{aligned}$$

Obviously the EDSR intensity approaches to zero when  $\gamma_1 = (\omega_c + \omega_z)\alpha / (\omega_c - \omega_z) \simeq 0.5\alpha$  for  $\phi = \pi/4$ . The dependence of the EDSR intensity on the direction of the  $ac$  electric field is plotted in Figure 6 in the R + D case.

## 5 Conclusion and discussion

We have analyzed the strain-assisted manipulation of electron spins in quantum wells where an in-plane  $ac$  electric field and a perpendicular magnetic field are applied. The strain effects on the manipulation of electron spins are different for different semiconductor quantum wells. We exhibited that the efficiency of manipulating electron spins can be enhanced by tuning the strain strength of samples. There are four combinations of the intrinsic and strain-induced spin-orbit couplings, namely, D + R, D + D, R + R and R + D. These four cases can provide different strain dependences of the EDSR intensities when the direction of the  $ac$  electric field is adjusted from  $\phi = \pi/4$  to  $\phi = 3\pi/4$ , and the strain strength is tuned in the EDSR experiments. The four kinds of combined effects of spin-orbit couplings are helpful for the efficient manipulation of electron spins and for understanding the

experimental phenomena brought in by the strain in some semiconductor quantum wells. It is worthwhile to mention that the spin-orbit coupling strengths including the Dresselhaus parameter  $\beta$  may depend on the magnetic field [32–35] under certain conditions. In order to present clearly the strain effects of the EDSR intensity, we have neglected the magnetic field dependence of the spin-orbit coupling strengths in this paper. Actually, the magnetic field dependence of the Dresselhaus parameter  $\beta$  can be neglected when the confinement in the  $z$  direction is sufficiently strong, namely  $(\omega_c/\omega_0)^2 \ll 1$ . It is reasonable to neglect the magnetic field dependence of the Dresselhaus parameter  $\beta$  due to the strong confinement considered in this paper.

The work was supported by NSFC grant No. 10674117 and by PCSIRT of the Ministry of Education of China (IRT 0754).

## References

- S.A. Wolf, D.D. Awschalom, R.A. Buhrman, J.M. Daughton, S. von Molnár, M.L. Roukes, A.Y. Chtchelkanova, D.M. Treger, *Science* **294**, 1488 (2001)
- S. Datta, B. Das, *Appl. Phys. Lett.* **56**, 665 (1990)
- J. Schliemann, J.C. Egues, D. Loss, *Phys. Rev. Lett.* **90**, 146801 (2003)
- I. Žutić, J. Fabian, S. Das Sarma, *Rev. Mod. Phys.* **76**, 323 (2004)
- D. Loss, D.P. DiVincenzo, *Rev. Rev. A* **57**, 120 (1998)
- Y. Kato, R.C. Myers, D.C. Driscoll, A.C. Gossard, J. Levy, D.D. Awschalom, *Science* **299**, 1201 (2003)
- E.I. Rashba, A.L. Efros, *Phys. Rev. Lett.* **91**, 126405 (2003); E.I. Rashba, A.L. Efros, *Appl. Phys. Lett.* **83**, 5295 (2003)
- A.L. Efros, E.I. Rashba, *Phys. Rev. B* **73**, 165325 (2006)
- Y. Kato, R.C. Myers, A.C. Gossard, D.D. Awschalom, *Nature (London)* **427**, 50 (2004); Y.K. Kato, R.C. Myers, A.C. Gossard, D.D. Awschalom, *Phys. Rev. Lett.* **93**, 176601 (2004)
- S.A. Crooker, D.L. Smith, *Phys. Rev. Lett.* **94**, 236601 (2005)
- M. Beck, C. Metzner, S. Malzer, G.H. Döhler, *Europhys. Lett.* **75**, 597 (2006)
- L. Jiang, M.W. Wu, *Phys. Rev. B* **72**, 033311(2005)
- M. Hruška, Š. Kos, S.A. Crooker, A. Saxena, D.L. Smith, *Phys. Rev. B* **73**, 075306 (2006)
- H. Knotz, A.W. Holleitner, J. Stephens, R.C. Myers, D.D. Awschalom, *Appl. Phys. Lett.* **88**, 241918 (2006)
- V. Sih, H. Knotz, J. Stephens, V.R. Horowitz, A.C. Gossard, D.D. Awschalom, *Phys. Rev. B* **73**, 241316(R) (2006)
- B.A. Bernevig, S.C. Zhang, *Phys. Rev. B* **72**, 115204 (2005)
- M.I. D'yakonov, V.Y. Kachorovskii, *Fiz. Tekh. Poluprov.* **20**, 178 (1986) [*Sov. Phys. Semicond.* **20**, 110 (1986)]
- J. Fabian, A.M. Abiague, C. Ertler, P. Stano, I. Žutić, *Acta Physica Slovaca* **57**, 565 (2007)
- W. Zawadzki, P. Pfeffer, *Semicond. Sci. Technol.* **19**, R1 (2004)
- E.I. Rashba, *Fiz. Tverd. Tela(Leningrad)* **2**, 1224 (1960) [*Sov. Phys. Solid State* **2**, 1109 (1960)]
- Yu.A. Bychkov, E.I. Rashba, *Pis'ma Zh. Eksp. Teor. Fiz.* **39**, 66 (1984) [*JETP Lett.* **39**, 78 (1984)]
- G.E. Pikus, A.N. Tikov, *Optical Orientation*, edited by F. Meier, B.P. Zakharchenya (North-Holland, Amsterdam, 1984), Vol. 8
- Z. Wilamowski, W. Jantsch, H. Malissa, U. Rössler, *Phys. Rev. B* **66**, 195315 (2002)
- W. Jantsch, Z. Wilamowski, N. Sandersfeld, M. Mühlberger, F. Schäffler, *Physica E* **13**, 504 (2002)
- P. Pfeffer, W. Zawadzki, *Phys. Rev. B* **41**, 1561 (1990)
- R. Lassnig, *Phys. Rev. B* **31**, 8076 (1985)
- W.K. Liu, X. Zhang, W. Ma, J. Winesett, M.B. Santos, *J. Vac. Sci. Technol. B* **14**, 2339 (1996)
- V.I. Perel', S.A. Tarasenko, I.N. Yassievich, S.D. Ganichev, V.V. Bel'kov, W. Prettl, *Phys. Rev. B* **67**, 201304(R) (2003)
- B.A. Bernevig, S.C. Zhang, *Phys. Rev. Lett.* **96**, 106802 (2006)
- R. Ranvaud, H.R. Trebin, U. Rössler, F.H. Pollak, *Phys. Rev. B* **20**, 701 (1979)
- D.G. Seiler, B.D. Bajaj, A.E. Stephens, *Phys. Rev. B* **16**, 2822 (1977)
- P. Pfeffer, *Phys. Rev. B* **55**, R7359 (1996)
- P. Pfeffer, W. Zawadzki, *Phys. Rev. B* **59**, R5312 (1998)
- P. Pfeffer, W. Zawadzki, *Phys. Rev. B* **68**, 035315 (2003)
- G. Lommer, F. Malcher, U. Roessler, *Phys. Rev. Lett.* **60**, 728 (1988)